Evaluation of the efficiency of water treatment by a solar heating and distillation system

E. C. Tarango Brito , C. E. Barrera Díaz , L.I. Ávila Córdoba , P. Balderas Hernández , D. A. Solís Casados

PII: S2667-0100(23)00014-8
DOI: https://doi.org/10.1016/j.envc.2023.100691
Reference: ENVC 100691

To appear in: *Environmental Challenges*

Received date: 2 November 2022
Revised date: 28 December 2022
Accepted date: 30 January 2023

Please cite this article as: E. C. Tarango Brito , C. E. Barrera Díaz , L.I. Ávila Córdoba , P. Balderas Hernández , D. A. Solís Casados , Evaluation of the efficiency of water treatment by a solar heating and distillation system, *Environmental Challenges* (2023), doi: https://doi.org/10.1016/j.envc.2023.100691

Evaluation of the efficiency of water treatment by a solar heating and distillation system

E. C. Tarango Brito[a], C. E. Barrera Díaz[b], L. I. Ávila Córdoba[c*], P. Balderas Hernández[d], D. A. Solís Casados[e]

[a, b, d] *Faculty of Chemistry, Autonomous University of the State of Mexico, Paseo Colón S/N, Residencial Colón y Ciprés, 50120, Toluca, State of Mexico, Mexico.*

[c*] *Faculty of Engineering, Autonomous University of the State of Mexico, Cerro de Coatepec S/N; 50100, Toluca, State of Mexico, Mexico.*

[e] *Joint Center for Research in Sustainable Chemistry, UAEM-UNAM, Carretera Toluca - Atlacomulco km. 14.5, Unidad San Cayetano, 50200 Toluca, State of Mexico, Mexico.*

*Corresponding author: liac07@gmail.com,

Graphical abstract

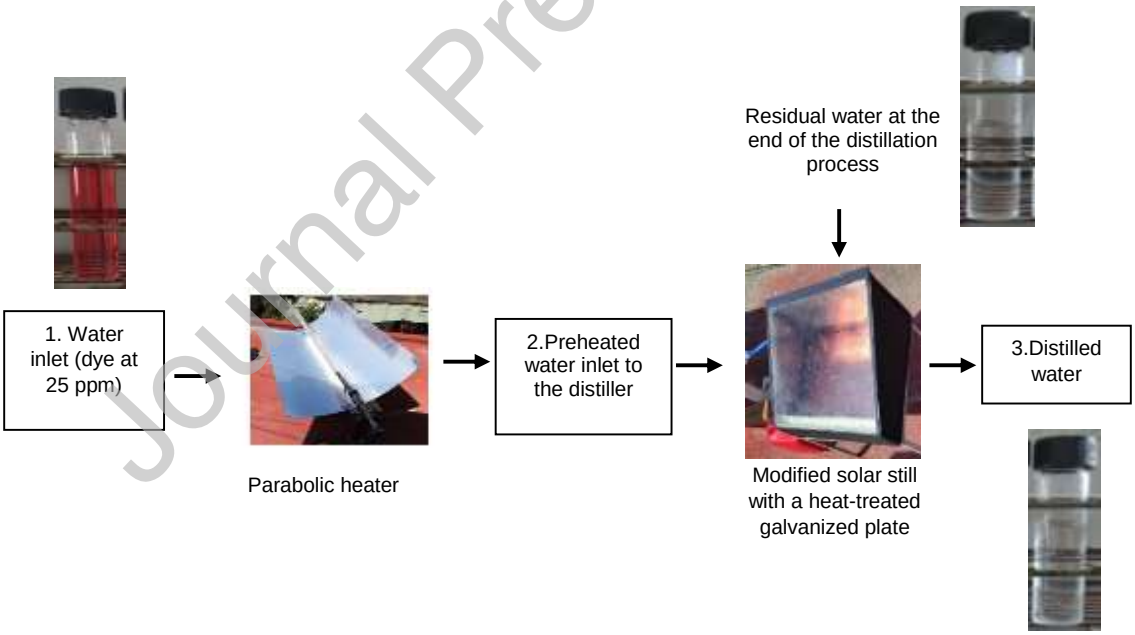

Abstract

Presently, many industries discharge colored wastewater without any treatment to water bodies such as rivers and lakes affecting flora and fauna. Due to its chemical composition, its self-purification in phreatic bodies is complicated. Although there are chemical, physical and biological treatments dedicated to the degradation of this type of compounds, they present economic and energetic disadvantages. This study reports the use of solar energy for the treatment of water containing carmine red dye at 25 ppm. The system consists of the coupling of two modules; the first heats wastewater using a parabolic heater, while the second separates clean

water (distilled) from pollutants. It was observed that when a galvanized ZnO plate is introduced into the distillation unit a photodegradation process takes place improving the characteristic of the concentrate. Optimal conditions allow an efficiency of 87% in the production of the distilled water obtained. Parameters such as pH, Conductivity, COD, Turbidity and Total Solids, indicate that the distilled water complies with the maximum permissible limits for water quality established in Mexican regulations. A 93-percent photodegradation of carmine red dye wastewater was detected within 120 min during the process, which was verified by UV-Vis and IR characterization.

Keywords: Photodegradation; Solar heating; Solar distillation; Carmine red; Galvanized ZnO plate.

1. Introduction

Anthropogenic activities generate severe impacts on water resources, freshwater availability on the planet is only 2.5% and 70% is not available for human consumption [1]. The presence of dyes as frequent water contaminants is of particular importance, since they are widely used in a variety of industries, such as textile, food, pharmaceutical, tanning, glass as well as those related to plastic manufacturing processes [2, 3]. Textile industry uses large amounts of artificial colorants in its dyeing processes, the problem is that few manufacturing facilities treat wastewater, and the majority discharges it without any treatment. Nowadays, it is estimated that the annual production of these compounds is around 700,000 t. [4].

The presence of dyes in wastewater is a challenge for traditional wastewater treatment since they have complex chemical structures, toxicity [5] and little or no biodegradability [2]. They also present high values of chemical oxygen demand (COD) and biological oxygen demand (BOD) [6]. For these reasons, new alternatives have been sought to recover drinking water in a more sustainable and friendlier way to the environment.

Solar distillation has proven to be an option to obtain pure water; it is a simple method, and has some advantages such as a simple manufacture, minimal need for work, and a virtually maintenance-free operation [7].

Furthermore, solar thermal collectors are devices that capture solar energy and convert it into useful heat energy at various temperatures [8]. In general terms, it is a heliothermal process in which a mass of water, contained in a vessel with a cover, is heated by the effect of solar radiation [9].

Up to the present, solar stills have been applied mainly for the desalination of seawater with the subsequent obtaining of fresh water. However, its application and usefulness to separate and photo-degrade pollutants (specifically dyes such as carmine red) has not been reported. Thus, in the present study, a coupled solar heating-distillation-photocatalyst system was used for treating wastewater in an easy low-cost way obtaining a 90% efficiency.

The novel device presented in this work uses solar energy for three purposes: heat wastewater, separate pollutants from water taking advantage of distillation, and degrade organic pollutants using a galvanized ZnO plate as a photocatalyst. Such device exclusively operates with renewable energy, which makes it sustainable and friendly to the environment; for its part, the treated water has high quality.

2. Material and methods

2.1 Preparation of synthetic wastewater with carmine red dye

A solution of distilled water with carmine red dye was prepared at a concentration of 25 ppm. 625 mg of the dye were weighed using an analytical balance and added into a volumetric flask.

2.2 Parabolic solar concentrator

The parabolic solar concentrator is based on a parabolic surface that concentrates the radiation on a receiver and allows heating the water. The objective of this device was to preheat the wastewater in order to transfer it at a high temperature to the distiller still [10].

2.3 Single slope solar still construction

The single-slope solar still was designed using measurements to allow for a maximum capacity of 10 L. The base and walls of the distiller were built with anodized aluminum (obtained from the company La Paloma Compañía de Metales S. A. de C. V.) and insulated with foam. The cover of the distiller had a float glass with a smooth flat surface and no optical distortion. The inlet consisted of a ¼" PVC pipe and a 1" gutter of the same material. The distilled water was collected with a pipeline and received in a container. Among the design parameters, a 20° slope was considered to achieve greater uptake of solar radiation and therefore higher temperature in the city of Toluca (located at a latitude of 19° 17' 29").

2.4 Evaluation of temperature and efficiency in the parabolic solar heater, in the still and in the coupled heating-solar distillation system

Several experiments were performed for temperature evaluation, particularly in winter and spring, in order to establish the optimal conditions that would allow obtaining a larger volume of distilled water.

In both cases, winter and spring, a sample of 1000 mL of distilled water was placed inside the parabolic solar heater and in the solar still at 9:00 am at an initial temperature of 14.0 °C, subsequently temperature measurements were taken every half an hour for 1 solar day (8 h), when the collected water was measured to determine the efficiency of the parabolic solar heater and the distiller. Carrying out the same procedure, a dye solution was placed to determine such parameter. In the case of the coupled system the same initial conditions were used.

The Solar heating and distillation systems were connected by means of a hose using 1" couplings to transfer the water. In this sense, 1000 mL of laboratory distilled water were introduced into the solar heater at 9:00 am. At 12:00 pm, the preheated water was transferred to the solar still where retention time was 5 h. Before sunset and at the end of the process, the collected water was measured in a test tube, to compare it with that obtained previously in the simple solar still. Moreover, by means of the same procedure, the evaluation was carried out with a solution of carmine red at 25 ppm. These experiments were run in winter and spring by triplicate.

2.5 Parameter optimization

Once the temperatures and the amount of distilled water obtained from all the processes were determined, different initial volumes of water V_0 = 1000, 750, 500 and 250 mL were tested.

In the first try, 1000 mL of laboratory water were introduced into the parabolic solar heater at an initial temperature (T_0) of 14.0 °C, once the selected temperature was reached (80 °C), the water was sent to the solar still to measure the volume of distilled water (Vf). The same procedure was performed using different initial water volumes of 750, 500 and 250 mL. These experiments were run in spring and winter.

2.6 Study of the photodegradation of carmine red dye from the coupled solar heating-distillation system

Once the optimal parameters for the coupled system were obtained, a treatment was carried out in order to determine the photo-degradation of this azo dye. To achieve the above, the solar heating and distillation device was assembled to form the coupled system, modifying it through the use of a galvanized plate; in this sense, two experiments were carried out:

a). Without a galvanized plate.

b). With a galvanized plate subjected to heat treatment carried out at a temperature of 500 °C for 2 hours in a Felisa brand muffle, model FE-361. This for the purpose of producing ZnO, since previous studies have verified it has photocatalytic properties [11].

The procedure consisted in introducing a solution of 250 mL of carmine red at To = 14.0°C into the solar heater until it reached 80°C, which took place at 11:00 am; then, it was transferred to the distiller, where the two aforementioned experiments were carried out. In this case, samples of the synthetic wastewater contained in the device were taken every half an hour for a period of 2 h, for their subsequent characterization using UV-VIS spectrophotometry model VE-5100UV at a wavelength range from 200 to 600 nm, and IR-ATR model TENSOR 21 at a wavenumber range from 500 to 4000 cm^{-1}.

Then, an evaluation of the quality of the residual and distilled water collected at the end of said treatment was carried out with the measurement of physicochemical parameters referred to below.

2.6.1 pH

It was determined following the guidelines of the NMX-AA-008 SCFI-2016 standard, using a Milwaukee m102 brand potentiometer, which was calibrated at values of 4.01 and 7.01. Subsequently, the measurement was made in the initial synthetic water (25 ppm of carmine red dye), distilled water and in the residue collected at the end of the process [12].

2.6.2 Conductivity

It was carried out according to the procedure established in the NMX-AA-093-SCFI-2000 standard by means of a Hanna conductivity meter model HI99301, which measures conductivity and total dissolved salts up to 20 mS/cm. The equipment was calibrated with a pattern of 12.88 mS/cm [13].

2.6.3 COD

This parameter was calculated by the foundation established in NMX-AA-030/2-SCFI-2011 [14] First, the heating plate was preheated at 150°C, then the sealed tubes or HACH vials (range 20-1500 mg/L) were shaken up to the homogenization of the content, proceeding in the same way with the samples to be analyzed, that is, the initial water at 25 ppm of carmine red dye, the treated distilled water and residual water collected at the end of the process. Subsequently, a volume of 2 mL was taken from each of them, which was placed in the vials, tightly capped, and the content was mixed by gently inverting the tube several times. Afterwards, the tubes were taken to the digester plate already preheated for 2 h. Once this time elapsed, they were removed and allowed to cool at room temperature to finally be read in the HACH DR/4000U brand UV-Vis spectrophotometer.

2.6.4 Turbidity

This parameter was evaluated following the NMX-AA-038-SCFI-2001 standard, samples were shaken vigorously in order to homogenize them and each one was placed in a cell of a HACH DR/4000U spectrophotometer [15].

2.6.5 Total solids

They were ascertained on the basis of NMX AA-034-SCFI-2015. First, three crucibles were placed in a Felisa oven, model FE-291 AD, for 20 min at 103-105 °C; then, they were cooled in a desiccator for 20 min and weighed on an analytical balance [16].

The oven-desiccator cycle was repeated until a difference ≤ 0.0005 g was obtained in two consecutive weighings (taking into account the last recorded weight value, considered P1). Subsequently, 50 mL of each of the samples to be analyzed were placed and taken to the oven for evaporation at a temperature between 100 and 105 °C. Afterwards, they were cooled in the desiccator for 20 min and finally weighed on an analytical balance (P2). Calculations were made using the following formula:

$$ST = (P1 - P2)/Sample\ Volume \quad (1)$$

Where:

ST= Total solids [mg/L]

P1= Constant weight of the crucible [mg]

P2= Weight of the dry residue plus the weight of the crucible [mg]

Sample volume [L]

2.6.6 UV-VIS Spectrophotometry

Initial and treated water samples were taken in order to determine the absence of carmine red dye by means of a VELAB spectrophotometer, model VE-5100UV UV-VIS.

2.7 Scanning electron microscopy (SEM)

The surface morphology of the wall covering was observed in both forms, using a scanning electron microscope model JEOL JSM-6510LV. Images were acquired with 250X.

2.8 X-ray photoelectron spectroscopy (XPS)

A sample of the wall covering was taken and characterized, in both forms, with and without galvanized plate, the atomic chemical composition of the surface and chemical bonding of the elements present was ascertained. The XPS spectra in the wide window were acquired using a source of Mg Kα line that has an energy of 1253.6 eV, from 50 to 1000 eV of binding energy, 50 eV of pass energy, dwell of 100 and 1 scan using a JEOL JPS 9200. The narrow spectra of each element were taken in the respective region with 20 eV of pass energy, dwell of 100 and 8 scans, using the 285eV position of the adventitious carbon peak to adjust and correct any shift due to the sample charge in the rest of elemental regions. The baseline was corrected using a Shirley-type model

2.9 Real wastewater treatment

Real residual water was taken from Lerma River, State of Mexico, at the coordinates 19° 16’ 38.1” N, 99° 31’ 22.2” W, where textile companies discharge wastewater. 1000 mL of actual residual water was collected and stored in a polyethylene terephthalate plastic container, then it was transported inside a cooler to preserve and keep it at a temperature of 4° C for further treatment.

In order to evaluate the efficiency of the ZnO plate as a function of the number of process cycles, four tests were carried out using a carmine red aqueous solution.

3. Results and Discussion

3.1 Evaluation of temperature effect

The temperature effect was evaluated in the parabolic solar heater, the distillation still and in the coupled system.

The effect of temperature as a function of the season of the year and how this affects the heating, distillation and coupled process is displayed in Figure 1. By and large, in spring the temperature of water is higher in all the setups regarding its quality. A detailed analysis is presented below.

Fig. 1a shows the temperature variation using laboratory distilled water and a carmine red dye solution in two different seasons: winter and spring. For both kinds of water, the best conditions are obtained in spring, since a higher temperature is reached as compared with winter.

Figure 1b shows the data obtained in the distillation treatment using laboratory distilled water and the carmine red solution. As observed in all cases, seasons have a major impact on the process. For instance, using laboratory distilled water in spring, temperature increases over time, reaching a maximum value of 56.6 °C at 13:00 p.m. Then there is a decrease to 40.5 °C, at the end of the process the distilled volume was collected and measured in a test tube, obtaining 157 mL out of a 1000 mL sample. On the other hand, in winter, the temperature has the same trend, however, a lower maximum temperature is reached (48.5 °C) with a subsequent decrease to 28.6 °C at 17:00 p.m. In this case, the final volume of distilled water obtained was 115 mL. Therefore, the efficiency obtained is greater in spring in comparison with winter (15.7 and 11.5%, respectively).

Figure 1c shows the data obtained with laboratory distilled water and a solution of carmine red at 25 ppm in the coupled system. In spring, for laboratory distilled water, 292 mL were obtained at the end of the process from 1000 mL of initial water, with an efficiency of 29.2%. This means that the process was improved by 13.5% in comparison with the distillation of water without preheating.

In this way, as shown in Fig. 1, the coupled system improves the yield of distilled water production due to solar preheating in the parabolic solar heater in comparison with a simple still (without coupling).

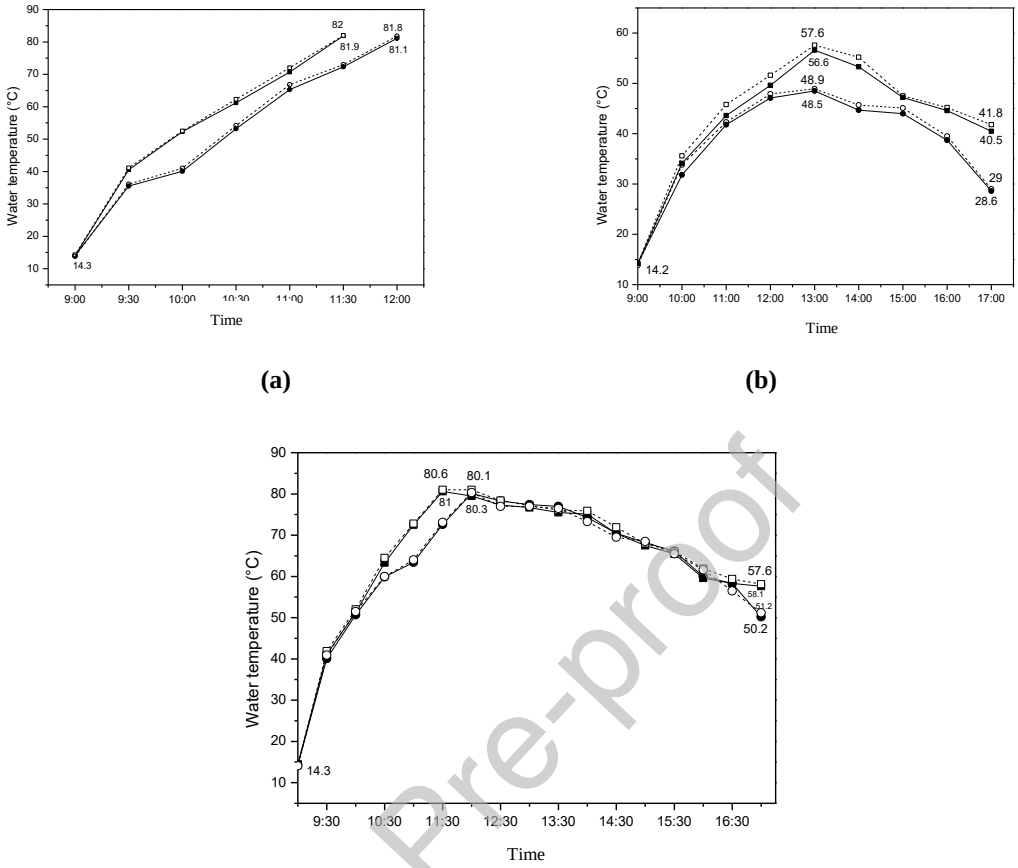

Fig. 1 Determination of temperature in (a) the parabolic solar heater, (b) solar still, and (c) coupled system. (--□--) water with dye in spring, (--○--) water with dye in winter, (—■—) laboratory distilled water in spring, (—●—) laboratory distilled water in winter.

3.2 Optimization of the operating parameters of the coupled solar heating-distillation system

With a view to improving the process, different initial water volumes were tested. Figure 2 shows that when the initial volume of water is 1000 mL, the amount of distilled water is around 30 %. As well, it is noticed that when the initial water volume decreases the amount of distilled water increases.

Therefore, it was possible to obtain the optimal parameter in the distiller to reach a maximum efficiency of 87% in the process in both seasons (the spring and winter of the year over which this project was carried out) using an initial water temperature (T_0) of 14.0 °C (at the entrance of the parabolic solar heater), an initial volume (V_0) of 250 mL, and a residence time (tr) of 5 h.

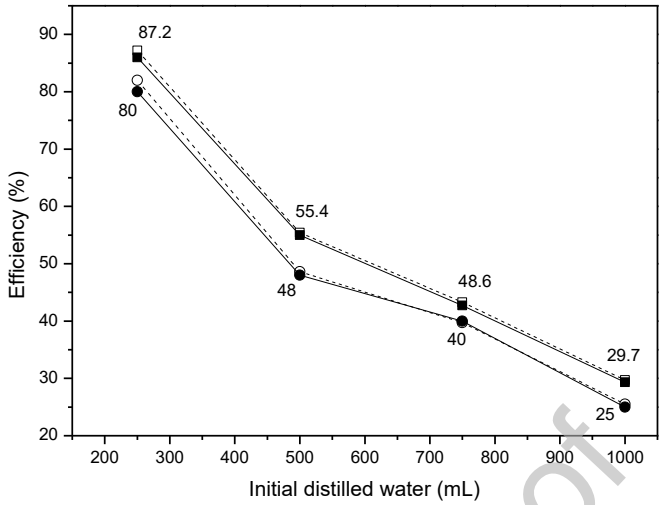

Fig. 2 Evaluation of the efficiency in a coupled solar heating-distillation system varying the initial volume of laboratory distilled water and of a solution of carmine red at 25 ppm in the process. (--□--) water efficiency with dye in spring, (--○--) water efficiency with dye in winter, (—■—) laboratory distilled water efficiency in spring, (—●—) laboratory distilled water efficiency in winter.

3.3 Photocatalytic process taking place during the distillation process

During the distillation process, solar sunlight is directly received by the carmine red solution for 5 hours. As described before, solar energy is used for evaporating water and separating it to obtain distilled water with good characteristics. However, as observed in Fig. 3a, the water containing carmine red dye absorbs at a wavelength of 503 nm. An interesting effect is that the absorption of the water samples increases over time because the concentration of the dye tends to increase due to distillation. The characteristic peak of the N=N chromophore group is observed at the 503 wavelength. In addition, the aromatic rings that appear in the range from 200 to 350 nm do not show any change, therefore, it is established there is no degradation of the compound.

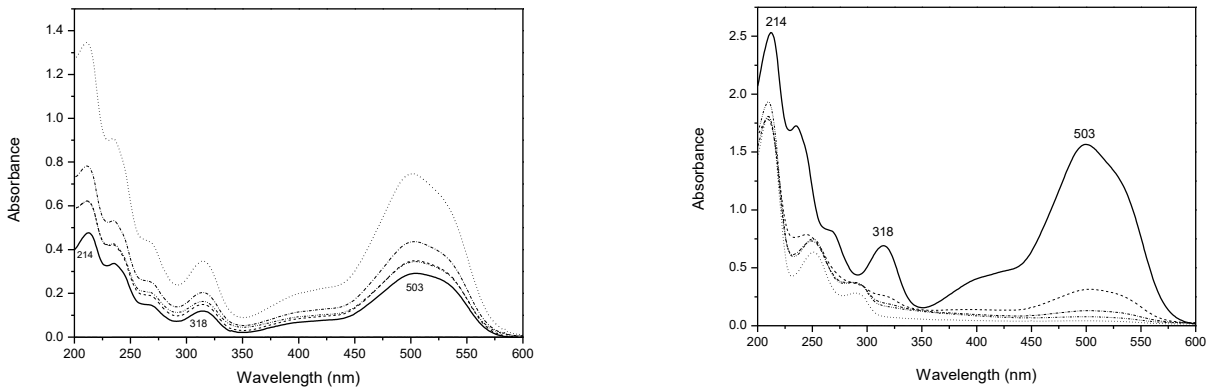

Fig. 3 UV-VIS spectrophotometry of water with carmine red dye, under treatment by a coupled solar heating-distillation system (a) without galvanized plate and (b) modified with a galvanized plate with heat treatment. (—) H_2O, (▬) initial 25 ppm, (- -) residue 11:30, (—·—) residue 12:00, (—··—) residue 12:30, (····) residue 13:00.

In order to improve the characteristics of the concentrated water, a ZnO plate (prepared in the lab) was introduced into the distillation unit. Fig. 3b shows the absorbance of carmine red in the visible region at 503 nm at the initial time of treatment by solar distillation. However, half an hour after starting the treatment, the peak decreased, and after another 30 min, it completely disappeared, indicating the total rupture of the nitrogen bond. On the other hand, new peaks are observed within a range from 200 to 300 nm, which shows the formation of aromatic amines and sulfonate groups that absorb in this region and that are degradation products of the dye; the same results have been reported previously.

A calibration curve was made to establish the final concentration of the treated solution and thus determine the percentage of photo-degradation. In this sense, it was registered that after 120 min of treatment the concentration drops from 25 to 1.76 ppm, with a percentage of photodegradation of the carmine red dye of 93 %.

3.4 IR-ATR spectroscopy

The structural analysis of the synthetic residual water of carmine red dye obtained after treatment under the modified coupled system with a thermally treated galvanized plate (as a photocatalyst) is presented in Figure 4. A strong absorption band is observed at 3306.34 cm^{-1} corresponding to the -OH group associated in the initial samples as well as in those taken at 11:30 am, 12:00 pm, 12:30 pm, and later at 13:00 h such bond is broken. On the other hand, an average stretch was obtained at 1633.33, in the same samples mentioned above, belonging to the C=C bond, which, in the final sample, is fractionated. Likewise, an absorption peak at 585.97 cm^{-1} of the $(SO_3)^{2-}$ bond is noticed, this bond is lost in the final sample taken during the treatment.

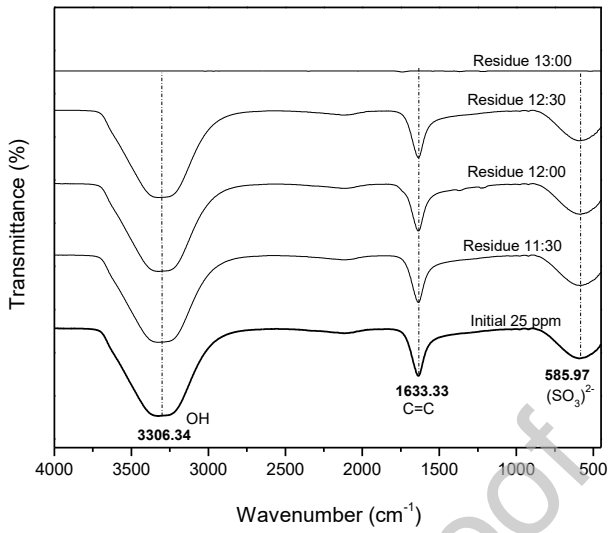

Fig. 4 IR-ATR spectroscopy of the synthetic residual water of carmine red dye, under treatment by a modified solar heating-distillation coupled system with a thermally treated galvanized plate.

3.5 UV-VIS Spectrophotometry

In Figure 5, it is seen that the initial sample of a dye solution at 25 ppm presents the characteristic peak of -N=N- of carmine red at 503 nm, however, the samples of distilled and residual water at end of the process do not exhibit such stretching. Therefore, once the treatment was carried out, the water samples do not present a colorant. Furthermore, as mentioned above, in the final residual water, the presence of aromatic amines and sulfonate groups is observed within a range from 300 to 200 nm.

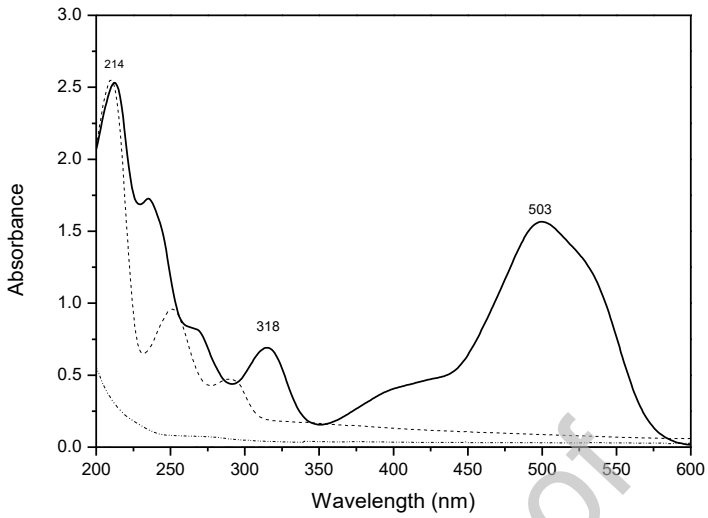

Fig. 5 UV-VIS spectrophotometry of residual and final treated distilled water by means of a coupled solar heating-distillation system with thermally treated galvanized plate. (─) H_2O, (▬) initial 25 ppm, (- -) treated wastewater, (— — —) treated distilled water.

3.6 Assessment of water quality

The quality of the distilled and residual water obtained at the end of the treatment was evaluated by means of the modified coupled system with the thermally treated galvanized plate, as displayed in Table 1

It is noticed that the initial and distilled water collected have a slightly acidic pH, while the final residual water has a neutral value. However, water after treatment is within the maximum permissible limit established in the NOM-127-SSA1-1994 standard (6.5 to 8.5) On the other hand, the electrolytic conductivity showed the same values for the initial water as in the obtained distilled water. While the residual water at the end of the process has a higher value, therefore, it is established there is a higher concentration of salts in it. After treatment, both types of water are within the established maximum permissible limit (1.5 mS/cm) [17].

Chemical oxygen demand (COD) showed that the initial sample has a similar value to the final residual water, while the distilled water obtained at the end of the process has a minimum value of 0.98; this makes its degree of biodegradability increase, therefore, purer water is obtained. The three types of water are within the maximum permissible limit (250 mg/L). It is noticed as well that the result of turbidity in the initial sample shows a value of 8. While for the treated wastewater, it increases to 33 owing to the concentration of salts from the dye. Regarding the treated distilled water, it presented a value under 5, which is within the maximum permissible limits established in the NOM-127-SSA1 standard of 1994. Finally, in total solids, it is observed that the final residual water sample has a higher amount of these as compared with the initial sample and the treated distilled water. However, the three types of water are within the maximum permissible limit of 100 mg/L, as established by the NOM-067-ECOL-1994 standard [17-19].

In general, it is observed that the quality of the distilled water obtained at the end of the treatment complies with the maximum permissible limits in all the physicochemical parameters evaluated. While the final residual water improves in quality, it has high turbidity, nevertheless.

Table 1. Water quality results obtained

Type of water	pH	Conductivity [mS/cm]	COD [mg/L]	Turbidity [UNT]	Total solids [mg/L]
Initial water (dye at 25 ppm)	6.31	0.03	37	8	0.016
Residual water at the end of the distillation process	7.06	0.12	47	33	0.076
Distilled water obtained	6.60	0.03	0.98	5	0.012

Dye degradation using conventional techniques presents favorable results. In 2018, Yslas studied the effect of sunlight and hydrogen peroxide on the degradation reaction to decolorize a carmoisine solution, using a new CuO-CoO catalyst supported on an aluminosilicate-zeolite matrix. The results show that a degradation of 8.4% is achieved with hydrogen peroxide and the catalyst without sunlight. A 21.3% is reached in the presence of sunlight. For the purpose of improving dye degradation, it was necessary to use hydrogen peroxide, the catalyst and sunlight [20].

Another approach is to use the Fenton reaction. In 2012, Arroyave et al. carried out the degradation of Ponceau Red dye at an initial concentration of 100 mg/L. Despite obtaining a high dye degradation efficiency (87 %), the process presents disadvantages such as pH control in acidic conditions (under 3.0) [21]

The use of TiO_2 as a photocatalyst was studied by Manrique et al. in 2017. Under the best conditions, i.e., 3 hours of sunlight and suspended TiO_2, a color degradation of 100% and 80% of COD were obtained. The main problem of this process is the use of suspended TiO_2 [22]. Other studies demonstrating the photocatalytic activity of ZnO were conducted by Rueda-Salaya (2017) and Flores-Moreno (2019) [23, 24].

As noticed in the present work, the photodegradation of carmine red obtained from a solar heated distillation system modified with a ZnO plate offers similar values as compared with some previous investigations, since a photodegradation of 93% is reached. Moreover, the advantages of this treatment are that it does not require the addition of chemicals over the process, and that high-quality distilled water is obtained using solar power.

3.7 Real wastewater

Using optimal parameters, 250 mL of real wastewater are placed into the solar heater, where it reaches 78.5° C, afterward wastewater is introduced into the distiller, where the distillation process takes place and wastewater reaches a final temperature of 40°C. At the end of the test, a volume of 138 mL of distilled water is obtained, which showed a similar efficiency value (65 %) in comparison with synthetic residual water.

The characteristics of treated and wastewater are shown in Table 2. Let us remark that the quality of the distilled water complies with the quality parameters established in Mexican regulations. In addition to this, the residual water at the end of the process shows favorable values except for turbidity, as it exceeded the maximum permissible limit [17-19].

Table 2. Results for water quality using real wastewater

Type of water	pH	Conductivity [mS/cm]	COD [mg/L]	Turbidity [UNT]	Total solids [mg/L]
Initial wastewater	7.14	1.02	42.4	67	0.030
Residual wastewater at the end of the distillation process	7.11	6.61	0	100	0.090
Distilled water obtained	6.99	0.31	0.5	1	0.016

In Figure 6a, a photograph of the original wastewater is shown. Figure 6b displays the concentrate; Figure 6c, the distilled water. It is important to restate that the proposed process works well with actual wastewater.

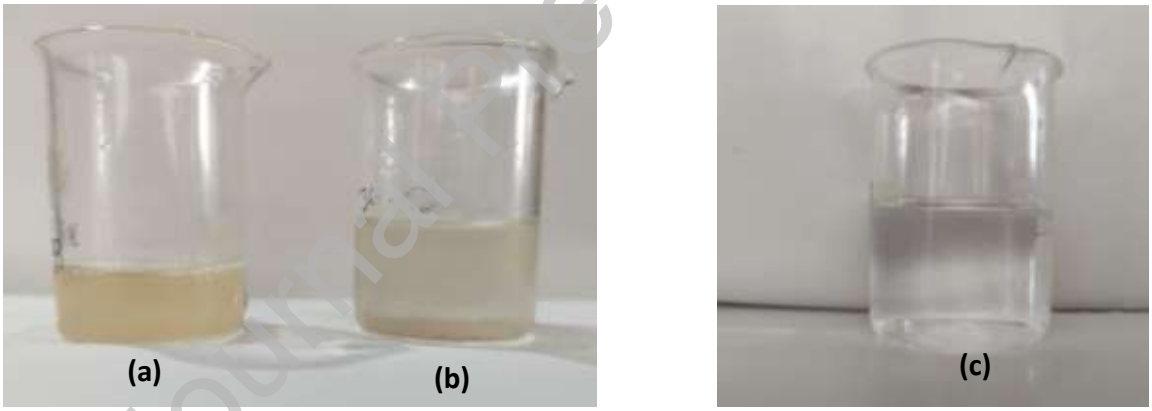

Fig. 6 (a) Real wastewater; (b) Residual wastewater at the end of the distillation process and (c) Distilled water obtained.

In order to assess the efficiency of the ZnO plate as a function of the number of process cycles, four tests were carried out using a carmine red aqueous solution. In all cases, a similar degradation efficiency was detected, while similar physicochemical characteristics of distilled and concentrated water were obtained. However, the surface of the plates changes in function of the process cycle as shown in Figure 7.

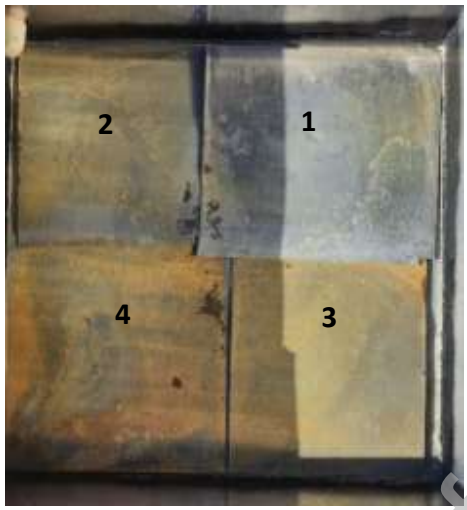

Fig. 7 ZnO surface after the photodegradation process for four cycles.

In plate number 1, a slight change in the color is observed after running the first cycle. This change in the plate increases as the following cycles run, up to cycle 4, when it is noticed that the plate is colored with residues of carmine red dye. Plus, two test were carried out with actual residual water, in which it was possible to notice that the plate is able to maintain the same photodegradation efficiency.

3.8 Characterization of the galvanized plate

3.8.1 SEM analysis

Figure 8 shows the morphological analysis by means of scanning electron microscopy (8a), and the electron dispersion analysis spectra (8b) corresponding to the galvanized sheet without heat treatment, and the morphological analysis by means of SEM (8c), and the EDS analysis (8d) corresponding to the galvanized sheet with heat treatment at 500°C. In Fig. 8a the surface of Zn coating is observed, additionally smooth areas and some regions with defect lines can be appreciated. Moreover, in Fig. 8b, the presence of Al and Fe was recorded, since they are the elements used as substrate, and Zn for galvanic coating; C and O are also observed, which are molecules adsorbed from the environment on the surface of the plate [11].

Fig. 8c shows the agglomeration and dispersion of ZnO particles on the surface of the plate. Besides, in Fig. 8d the presence of the elements used as substrate was recorded; C and O absorbed by the plate from the treatment which it was subjected to are also noticed.

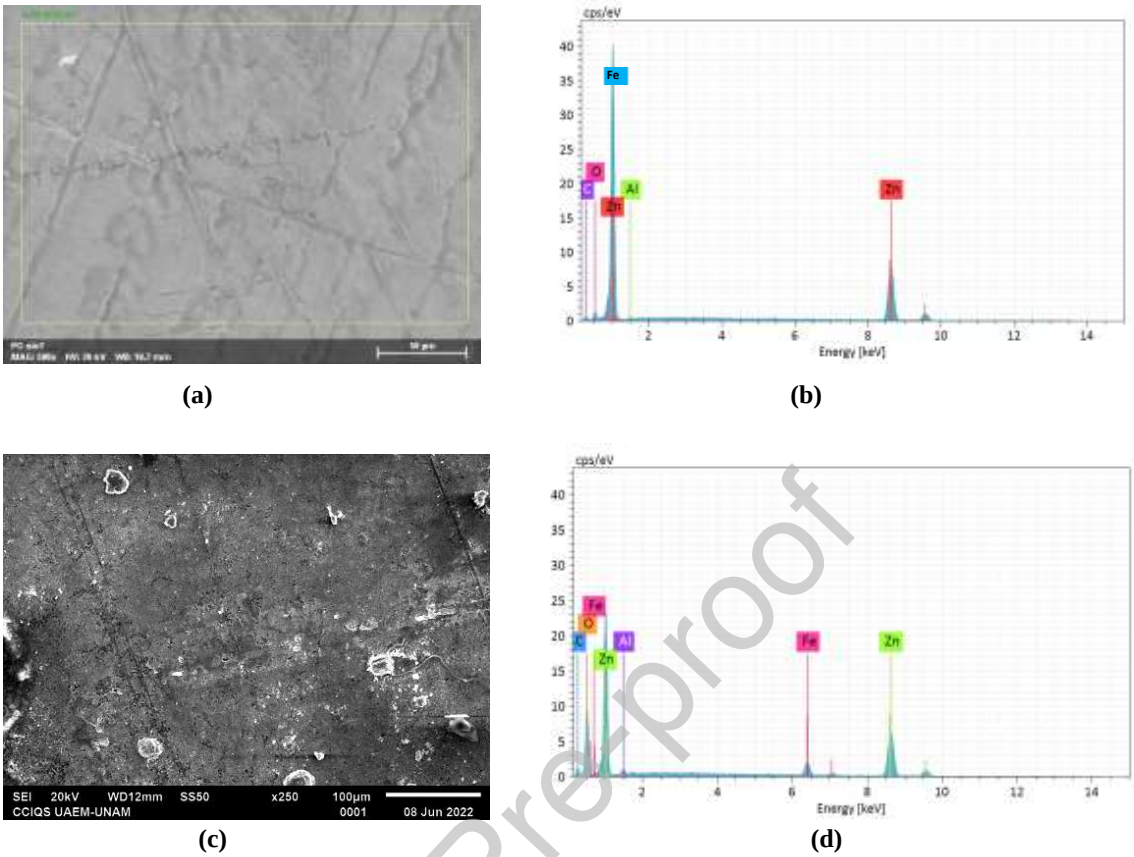

Fig. 8 (a) SEM micrograph and (b) EDS spectrum of the galvanized sheet without heat treatment. (c) SEM micrograph and (d) EDS spectrum of the galvanized sheet with heat treatment.

3.8.2 Analysis by XPS

The XPS spectra of the untreated and thermally treated galvanized sheet are shown in Figure 9 (a, b, c) for regions Zn 2p, C1s, and O 1s, respectively. Region Zn 2p is shown in Fig. 9a, the main finding in this region is that the treated sample has a slight shift from 1023 eV to lower binding energies such as 1020 eV after treatment, which was associated with a higher degree of oxidation of the chemical environment of Zn; some authors refer to this displacement as oxygen-rich ZnO. This concurs with a report by Rueda Salaya, 2017, which established the Zn2p doublet at 1023 and 1046 eV for $Zn2p_{3/2}$ and $Zn2p_{1/2}$, respectively that are attributed to a 2^+ oxidation state of zinc. Likewise, Tirado et al., 2019, report Zn2p orbitals peaking at 1020.98 and 1044.88 eV.

Figure 9b displays the characteristic peak of oxygen at 532.8 eV, the increase in the amount of this in the plate with heat treatment, from what was reported by Flores, 2019, is assigned to the O^{2-} ions in the Zn-O bond, which can be elucidated from the peak broadening. This spectrum of the O1s region may have the contribution from several chemical environments of the oxygen.

In another sense, Fig. 9c shows a peak from 271 to 297 eV, which is associated with carbon, peaking at 285 eV, and its broadening is observed in the plate with heat treatment in comparison with the initial plate. This broad C1s peak also can be related to the report by Flores, 2019, in this peak, adventitious carbon is found at 285 eV as well as the contribution of another chemical environment of carbon assigned to the carbonyl (C=O) bond, which causes the distortion of the peak.

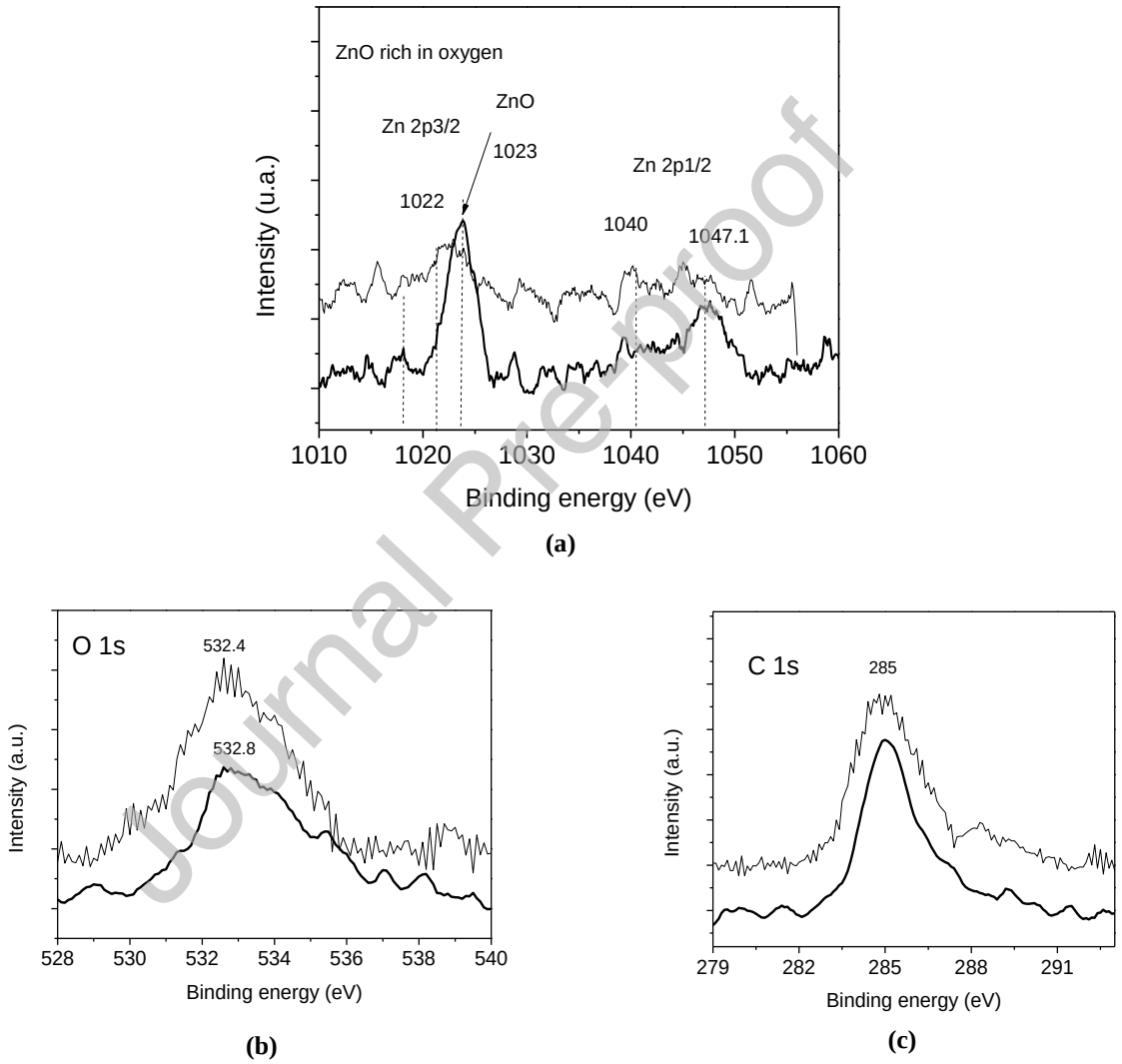

Fig. 9 General XPS spectrum for the galvanized plate with and without heat treatment. (a) carbon (C), (b) oxygen (O), (c) zinc (Zn). (▬) without heat treatment, (─) with heat treatment.

Conclusions

A parabolic water heater system was used in the present study in order to heat wastewater, at once the effect of spring and winter were evaluated, as it is important to demonstrate that this kind of process can be carried out throughout the year. A simple solar distillation process was used for separating high-quality clean water (distilled) and a concentrate. The results indicate that if only a simple solar distillation process is used, there is a distillation efficiency of 16.1%. However, when using a coupled solar warm-distillation system, the distillation improves the efficiency obtained by 13.5%, reaching a total of 29.2%

When an initial wastewater volume of 250 mL and an initial water temperature of 14.0 °C are used, the final efficiency reached is 87%. By introducing a ZnO plate into the distillation still, a 93-precent photodegradation of the dye is noticed within 2 h.

At the end of the process, in the assessment of the parameters of pH, conductivity, COD, turbidity and total solids, the treated photodegraded distilled water complies with characteristics defined by quality standards.

Acknowledgments

The financial support for this research from the National Council of Science and Technology of Mexico (CONACYT), as well as the Faculty of Chemistry of the Autonomous University of the State of Mexico (UAEM) and the Joint Center for Research in Sustainable Chemistry UAEM-UNAM.

Declarations of competing interest

The authors declare that they have no known competing financial interests or personal relationships that could have appeared to influence the work reported in this paper

References

1. Conagua (Comisión Nacional del Agua). (2016). Estadísticas del Agua en México 2016. Recuperado el 20 de abril de 2018 de: http://www.agua.unam.mx/assets/pdfs/novedades/EstadisticasdelAguaMexico2016_CONAGUA.pdf

2. Gebhardt, B. Sperla, R. Carle, R. & Müller-Maatsch, J., (2020), Assesing the sustainability of natural and artificial food colorants. Journal of Cleaner Production. 260, 120884, 1-10.

3. Lutamyo, N. A. Venant, H. L. Quintino, M. A., (2020), review on source, chemistry, green synthesis and application of textile colorants. Journal of Cleaner Production, 246, 1-13.

4. Zaruma Arias, P. E., Proal Nájera, J. B., Chaires Hernández I., Salas Ayala, H. I., (2018), Los colorants textiles industrials y tratamientos óptimos de sus efluentes de agua residual: una breve revision. Revista de la Facultad de Ciencias Químicas, ISSN: 1390-1869 N° 19, p.p.38-47.

5. HoosonI, J. GauntIda, Kiss, S. GrassoK, P. Butterworth, R., (1975), Long-term toxicity of indigo carmine in mice. Food and Cosmetics Toxicology.13 (2), 167-176.

6. Crespi M., (1999), tratamientos de aguas residuales del sector textil, Revista Galaxia 164, 1999-3, 49-53.

7. Yonny, F., Fasoli, H., Giai, M., Álvarez, H., (2008), Estudio de la biodegradabilidad y ecotoxicidad sobre colorants textiles, Hig. Sanid. Ambient. 8: 331-334.

8. Durkaieswaran, P. & Kalidasa Murugavel, K., (2015), Various special designs of single basin passive solar still – A review. Renewable and Sustainable Energy Reviews. 49, 1048–1060.

9. Chávez Sánchez, C. A., (2018), Estudio de la actividad fotocatalítica de colorantes en nanopartículas de cobre en ZnO, Tesis Profesional, Universidad de Sonora, departamento de ingeniería química y metalurgia, p.p. 1-42.

10. Ramírez, I. O., (2020), Acondicionamiento térmico doméstico mediante concentración solar por direccionamiento automático este-oeste. Tesis Profesional. Ingeniería en Sistemas Energéticos Sustentables. Facultad de Ingeniería. UAEM.

11. Ballesteros Balbuena M., Roa Morales G., Vilchis Nestor A. R., Castrejón Sánchez V. H., Vigueras Santiago E., Balderas Hernández P., Barrera Díaz C., Camacho López S., Camacho López M., (2020), Photocatalytic urchic-like and needle-like ZnO nanostructures synthetized by termal oxidation, Materials Chemistry and Physics, 244, 1-7.

12. NMX-AA-008-SCFI-2016 “Análisis de agua. - medición del pH en aguas naturales, residuales y residuales tratadas. - método de prueba”. Diario Oficial de la Federación. México.

13. NMX-AA-093-SCFI-2000 “Determinación de la conductividad electrolítica - método de prueba”. Diario Oficial de la Federación. México.

14. NMX-AA-030/2-SCFI-2011 “Determinación de la demanda química de oxígeno en aguas naturales, residuales y residuales tratadas - método de prueba - parte 2 - determinación del índice de la demanda química de oxígeno – método de tubo sellado a pequeña escala”. Diario Oficial de la Federación. México.

15. NMX-AA-038-SCFI-2001 “Análisis de agua – determinación de turbiedad en aguas naturales, residuales y residuales tratadas – método de prueba “. Diario Oficial de la Federación. México.

16. NMX-AA-034-SCFI-2015 “Análisis de agua - medición de sólidos y sales disueltas en aguas naturales, residuales y residuales tratadas – método de prueba”. Diario Oficial de la Federación. México.

17. NOM-127-SSA1-1994 "Salud ambiental, agua para uso y consumo humano-límites permisibles de calidad y tratamientos a que debe someterse el agua para su potabilización". Diario Oficial de la Federación. México

18. NOM-001-SEMARNAT-2021 “Límites permisibles de contaminantes en las descargas de aguas residuales”. Diario Oficial de la Federación. México.

19. NOM-067-ECOL-1994 “Límites máximos permisibles de contaminantes en las descargas de aguas residuales a cuerpos receptores provenientes de los sistemas de alcantarillado o drenaje municipal”. Diario Oficial de la Federación. México.

20. Yslas, K. (2018). Study of the effect of sunlight and hydrogen peroxide on the degradation of a dye using a copper and cobalt catalyst. Autonomous Mexico State University 1-69. Retrieved from: http://ri.uaemex.mx/handle/20.500.11799/95345. In December 2022.

21. Arroyave Rojas, J. A., Rodríguez Gaviria E. M., Barón Artizábal, A., Moreno Salazar, C. C., (2012), Degradation and mineralization of the red dye using Fenton's reagent, 2012; pp. 48 -58. ISSN 1909-0455.

22. Manrique, E. 2003. Photosynthetic pigments, something more than light capture. Spanish Association of Terrestrial Ecology, Ecosystems 2003/1, pp. 1-11. Retrieved from: https://www.revistaecosistemas.net/index.php/ecosistemas/article/view/250. In December 2022.

23. Rueda Salaya, L., (2017), Degradación fotocatalítica solar de diclofenaco mediante óxido de zinc modificado con fluoruro, Tesis Profesional, Facultad de Ciencias Químicas, Universidad Autónoma de Nuevo León, pp. 1-98.

24. Flores Moreno, A., (2019), Estudio de nanoestructuras de ZnO estabilizadas con polímeros, Tesis Profesional, Instituto de Ciencias Básicas e Ingeniería, Universidad Autónoma del Estado de Hidalgo, pp. 1-50.